

*Immunopathology and Infectious Disease*

# Protection against Human Immunodeficiency Virus Type 1 Tat Neurotoxicity by *Ginkgo biloba* Extract EGb 761 Involving Glial Fibrillary Acidic Protein

Wei Zou,<sup>\*†</sup> Byung Oh Kim,<sup>‡</sup> Betty Y. Zhou,<sup>\*</sup>  
Ying Liu,<sup>\*</sup> Albee Messing,<sup>§</sup> and Johnny J. He<sup>\*†¶||</sup>

From the Department of Microbiology and Immunology,<sup>\*</sup> the Center for Acquired Immune Deficiency Syndrome Research,<sup>†</sup> and the Walther Oncology Center,<sup>¶</sup> Indiana University School of Medicine, Indianapolis, Indiana; the Walther Cancer Institute,<sup>||</sup> Indianapolis, Indiana; the Department of Comparative Biosciences,<sup>§</sup> University of Wisconsin–Madison, Madison, Wisconsin; and the Department of Applied Biology,<sup>‡</sup> College of Life Science and Natural Resource, Sangju National University, Sangju, Republic of Korea

**Human immunodeficiency virus (HIV)-1 Tat protein is an important pathogenic factor in HIV-associated neuropathogenesis. Despite recent progress, the molecular mechanisms underlying Tat neurotoxicity are still not completely understood. However, few therapeutics have been developed to specifically target HIV infection in the brain. Recent development of an inducible brain-specific Tat transgenic mouse model has made it possible to define the mechanisms of Tat neurotoxicity and evaluate anti-neuroAIDS therapeutic candidates in the context of a whole organism. Herein, we demonstrate that administration of EGb 761, a standardized formulation of *Ginkgo biloba* extract, markedly protected Tat transgenic mice from Tat-induced developmental retardation, inflammation, death, astrogliosis, and neuron loss. EGb 761 directly down-regulated glial fibrillary acidic protein (GFAP) expression at both protein and mRNA levels. This down-regulation was, at least in part, attributable to direct effects of EGb 761 on the interactions of the AP1 and NF- $\kappa$ B transcription factors with the GFAP promoter. Most strikingly, Tat-induced neuropathological phenotypes including macrophage/microglia activation, central nervous system infiltration of T lymphocytes, and oxidative stress were significantly alleviated in GFAP-null/Tat transgenic mice. Taken together, these results provide the first evidence to support the potential for clinical use of EGb 761 to treat HIV-associated neurological diseases. More-**

**over, these findings suggest for the first time that GFAP activation is directly involved in Tat neurotoxicity, supporting the notion that astrocyte activation or astrogliosis may directly contribute to HIV-associated neurological disorders. (Am J Pathol 2007, 171:1923–1935; DOI: 10.2353/ajpath.2007.070333)**

Human immunodeficiency virus type 1 (HIV-1) infects the central nervous system, causing a variety of neuropathologies and neurobehavioral deficits. Common HIV-1 neuropathologies include astrogliosis, multinuclear giant cell formation, increased permeability of the blood-brain barrier, and neuron loss.<sup>1</sup> Memory loss, loss of motor control, and cognitive deficiencies often ensue.<sup>2,3</sup> A number of studies have shown that HIV-1 Tat protein is an important neuropathogenic factor that contributes to HIV-associated neurological diseases including dementia. The proposed mechanisms for Tat neurotoxicity include direct depolarization of neurons, increased levels of intracellular calcium, increased production/release of proinflammatory cytokines, increased infiltration of macrophages/monocytes, activation of excitatory amino acid receptors, and increased apoptosis.<sup>4</sup> Despite the significant progress made during the last few years, it is evident that our understanding of the molecular mechanisms underlying Tat neurotoxicity is still rapidly evolving.

Currently, no therapeutics have been developed to specifically target HIV-associated neurological disorders. Since introduction of highly active antiretroviral therapy in 1995,

---

Supported by the National Institutes of Health (grants R01NS039804, R01MH065158, and R21DA022986 to J.J.H.; and grants P01NS42803 to A.M. and P30HD033352 to the Waisman Center for development of congenic strains of the GFAP-null mice).

Accepted for publication September 4, 2007.

Supplemental material for this article can be found on <http://ajp.amjpathol.org>.

Present address of B.Y.Z.: Whitehead Institute for Biomedical Research, Cambridge, Massachusetts.

Address reprint requests to Johnny J. He, Department of Microbiology and Immunology, Indiana University School of Medicine, R2 302, 950 W. Walnut St., Indianapolis, IN 46202. E-mail: [jjhe@iupui.edu](mailto:jjhe@iupui.edu).

highly active antiretroviral therapy has dramatically improved the outlook for HIV-positive patients. With increased life expectancy, the prevalence of HIV-associated cognitive and neurological impairment is actually rising despite highly active antiretroviral therapy.<sup>5,6</sup> A number of therapeutic agents have been tried to target pathological sequelae of HIV neurological infection, ranging from the pain associated with peripheral neuropathology to neuron dysfunction and death, but few have been approved for clinical use. Thus, it is necessary to explore alternative strategies for treating HIV-associated neurological diseases.

Herbal products account for a substantial portion of the current interest in alternative treatments, and *Ginkgo biloba* extract (EGb) figures prominently in this interest. EGb possesses neuroprotective activity in animal models of neurodegenerative diseases<sup>7</sup> and ischemia.<sup>8</sup> EGb has been considered as a polyvalent therapeutic agent in the treatment of disturbances of multifactorial origin, including cerebral insufficiency,<sup>9</sup> mild cognitive impairments in elderly patients,<sup>10</sup> Alzheimer's disease, and vascular dementia.<sup>11,12</sup> Patients have displayed good tolerance for EGb, with no verified adverse drug interactions.<sup>11</sup> EGb has become the most widely sold phytomedicine in Europe and 1 of the 10 best-selling herbal medications in the United States.<sup>13</sup> One of the proposed mechanisms for the neuroprotective functions of EGb is that it protects neurons from LRP ligands such as occur in  $\beta$ -amyloid peptide-induced neurotoxicity.<sup>14,15</sup> Our recent studies suggest that interaction of HIV-1 Tat protein with LRP, with resulting disruption of the normal metabolic balance of LRP ligands, may contribute to AIDS-associated neuropathology including dementia.<sup>16</sup> These findings raise the possibility of using EGb as an alternative strategy to treat HIV-induced neurological disorders.

With recent development of a doxycycline (Dox)-inducible and brain-targeted HIV-1 Tat transgenic mouse model, we have shown that Tat expression in the brain resulted in neuropathologies reminiscent of several hallmarks noted in the brain of AIDS patients.<sup>17</sup> The small rodent model not only offers an opportunity to define further the molecular mechanisms of Tat neurotoxicity but also provides a platform to develop and validate therapeutic candidates targeted at HIV-associated neurological diseases. Therefore, in the present study, we determined the effects of EGb 761 against Tat-induced neurotoxicity in this unique neuroAIDS model.

## Materials and Methods

### Cell Cultures, Transfection, EGb 761 Treatment, and Reporter Gene Assay

Human astrocytoma U373.MG cells were purchased from the American Type Culture Collection (Manassas, VA). U373.MG cells stably expressing HIV Tat protein (U373.Tat) have been described elsewhere.<sup>18,19</sup> These cells were maintained in Dulbecco's modified Eagle's medium, supplemented with 10% fetal bovine serum, 50 U/ml penicillin, and 50  $\mu$ g/ml streptomycin, in a 37°C, 5% CO<sub>2</sub> incubator. For transfection, cells were plated in a six-well plate at a

density of  $3 \times 10^5$  cells/well, and the cells were then transfected with a luciferase reporter plasmid using Lipofectamine (Invitrogen, Carlsbad, CA). A CMV $\beta$ Gal plasmid (Clontech, Mountain View, CA) was included as a control to normalize variations among transfections. Transfected cells were then cultured for 2 days in the presence of EGb 761 at 0 to 200  $\mu$ g/ml, or its purified components terpene bilobalide and ginkgolide B at equivalent composition percentages (Ipsen Laboratories, Paris, France),<sup>20,21</sup> and harvested for the luciferase reporter gene assay using a luciferase assay system (Promega, Madison, WI). EGb 761 is extracted from green leaves of the *Ginkgo biloba* tree to a formulation of 24% flavonoids, 6% terpenes (eg, ginkgolides and bilobalide), 5 to 10% organic acids, and <0.5% proanthocyanidins.<sup>22</sup> A human glial fibrillary acidic protein (GFAP) promoter-driven luciferase reporter plasmid was obtained from Dr. Michael Brenner of the University of Alabama at Birmingham, Birmingham, AL,<sup>23</sup> and pNF $\kappa$ B-luc and pAP1-luc reporter plasmids were purchased from Clontech.

### Animals and Treatments

The animals were housed in the Laboratory Animal Care Center of Indiana University School of Medicine with a 12-hour light and 12-hour dark photoperiod. Water and food were provided *ad libitum*. All animal procedures were approved by the institutional biosafety committee. Tat transgenic mice and GFAP-null mice were previously generated.<sup>17,24</sup> The GFAP-null mice used for these experiments are congenic in a C57BL/6J background. Combination GFAP-null/Tat mice were obtained by standard cross-breeding using a higher Tat-expressing line Tg 271.<sup>17</sup> Progeny carrying both the GFAP-null alleles and Tat transgene were identified by PCR analysis of genomic DNA, which was extracted from mouse tail clippings (0.5 to 1 cm long) using the Wizard genomic DNA isolation kit (Promega). For amplification of the GFAP-Tet-on transgene, the primers 5'-GCTCCACCCCTCAG-GCTATTCAA-3' and 5'-TAAAGGGCAAAAGTGAGTATG-GTG-3' were used, whereas the TRE-Tat86 transgene was amplified with the primers 5'-GTCGAGCTCGGTAC-CCGGGTC-3' and 5'-CGGGATCCCTATTCCTTCGGGC-CTGT-3'. For the GFAP-null and wild-type alleles, the primers were 5'-CGAGAACCGAGCTGGAGTCT-3', 5'-TGGGCAAGACTGGTCATCTA-3' and 5'-AAGCGCATGC TCCAGACTGC-3'. Fifty ng of genomic DNA was used in the PCR reactions, with a program of 1 cycle of 94°C for 3 minutes, 35 cycles of 94°C for 1 minute, 60°C for 1 minute, and 72°C for 1 minute, and 1 cycle of 72°C for 7 minutes for TRE-Tat and GFAP-tet-on transgene amplification and a program of 1 cycle of 95°C for 3 minutes, 31 cycles of 95°C for 40 seconds, 61°C for 30 seconds, and 72°C for 2 minutes, and 1 cycle of 72°C for 5 minutes for GFAP-null and wild-type allele amplification. The expected sizes of the amplified fragments for GFAP-tet-on and TRE-Tat86 transgenes and GFAP-null and wild-type GFAP allele were 467 bp, 424 bp, 80 bp, and 310 bp, respectively. Mice at postnatal day 21 (P21) were given Dox (Sigma, Louis, MO) once a day via intraperitoneal

injection in a volume of 100  $\mu$ l at a dosage of 80 mg/kg/day for 7 days.<sup>17</sup> In case of EGb 761 treatment, unless stated otherwise, mice were given EGb 761 once a day intraperitoneally for an additional 7 days at a dosage of 100 mg/kg/day, which has been widely used in similar studies, or its purified components terpene bilobalide and ginkgolide B at equivalent composition percentages.<sup>25</sup> All animals were assigned to each experimental group in a random manner. Mice were monitored on a daily basis for growth (weight) and survival. Mice were sacrificed at the last day of the treatment, and the brains were harvested and divided sagittally. The hemi-brain was fixed at least 3 days in phosphate-buffered saline (PBS)-buffered 4% paraformaldehyde and processed for paraffin embedding. In all experiments, unless stated otherwise, comparisons were made between mice treated with Dox or vehicle control (water) and between mice treated with EGb 761 or vehicle control (PBS).

### *Hematoxylin and Eosin (H&E) Staining and Immunohistochemical Staining*

To ensure objective assessments and reliability of results, brain sections from mice to be compared in any given experiment were processed in parallel and examined by three independent individuals. H&E and immunohistochemical staining were performed as previously described.<sup>17</sup> For immunohistochemical staining, 10- $\mu$ m paraffin sections were cut on a microtome and mounted directly on glass slides. The sections were then deparaffinized in xylene and rehydrated and then stained using a Vectastain ABC kit (Vector Laboratories, Burlingame, CA) or a Dakocytomation ARK kit (for MAP-2 staining; DAKO, Carpinteria, CA) according to the manufacturer's instructions. The sources of antibodies were rabbit polyclonal anti-GFAP (1:500) and rabbit anti-CD3 (1:600) from DAKO, mouse anti-MAP-2 (1:100) from Santa Cruz Biotechnologies (Santa Cruz, CA), rabbit anti-Iba-1 (1:1000) from Wako Chemicals (Richmond, VA), and rabbit anti-S100 $\beta$  (1:1000) from Swant Biotech (Bellinzona, Switzerland). Omission of the primary antibodies was included as a control to evaluate nonspecific staining. Sections were examined, and bright-field microscopic images were captured with a Zeiss digital color camera mounted on an Axiovert M200 microscope (Zeiss, Thornwood, NY) using a  $\times$ 10 or  $\times$ 40 plan apochromat objective.

### *In Situ Apoptosis TUNEL Staining*

Ten- $\mu$ m paraffin brain sections were deparaffinized and rehydrated. Apoptosis was evaluated with the terminal deoxynucleotidyl transferase (TdT)-mediated dUTP nick end-labeling (TUNEL)-based TdT-FragEL DNA fragmentation detection kit (EMD Biosciences, La Jolla, CA). Briefly, deparaffinized sections were treated in 10 mmol/L of Tris-HCl, pH 8.0, containing 20  $\mu$ g/ml of proteinase K at room temperature for 20 minutes, and in 3% H<sub>2</sub>O<sub>2</sub> at room temperature for 5 minutes. Sections were then equilibrated with 1 $\times$  TdT buffer, and incubated with the TdT-labeling reaction mixture at 37°C for 1.5 hours. The labeling reaction was

terminated by addition of the stop solution supplied in the kit and incubated at room temperature for an additional 5 minutes. Sections were rinsed with TBS (20 mmol/L Tris-HCl, pH 7.6, and 140 mmol/L NaCl) between steps. Finally, apoptosis was visualized via incubation of the sections in 3, 3'-diaminobenzidine at room temperature for 15 minutes. Counterstaining was performed in 0.3% methyl green solution after a thorough rinse with distilled water.

### *Western Blot Analysis and Semiquantitative Reverse Transcriptase (RT)-PCR*

For Western blot analysis, U373.MG cells or U373.Tat cells were treated with EGb 761 at a concentration between 0 and 200  $\mu$ g/ml for 3 days and then washed twice to remove EGb 761 in ice-cold PBS, pelleted, and lysed in RIPA buffer (150 mmol/L NaCl, 1.0% Nonidet P-40, 0.1% sodium dodecyl sulfate, 50 mmol/L Tris-HCl, pH 8.0). Protein concentration was determined using a DC protein assay kit (Bio-Rad, Hercules, CA). Whole-cell lysates of 25  $\mu$ g of protein were electrophoretically separated by 12% sodium dodecyl sulfate-polyacrylamide gel electrophoresis and then electrotransferred to the HyBond-P membrane (Amersham, Piscataway, NJ). Proteins on the membrane were detected with primary antibodies and appropriate peroxidase-labeled secondary antibodies followed by the ECL chemiluminescence reagents (Amersham). Anti-mouse-GFAP antibody and anti-mouse  $\beta$ -actin antibody were both from Sigma. To determine GFAP mRNA levels, total RNA was isolated using the Trizol reagents (Invitrogen) according to the manufacturer's instructions, and subjected to RT-PCR using a Titan one-tube RT-PCR system kit (Boehringer Mannheim, Indianapolis, IN) with GFAP-specific primers (5'-AAGCAGATGAAGCCACCCTG-3' and 5'-GTCTGCACGGGAATGGTGAT-3'). RT-PCR was performed on a PE Thermocycler 9700 (PE Applied Biosystems, Foster City, CA) with a program of 50°C for 30 minutes, 94°C for 3 minutes, followed by 25 cycles of 94°C for 1 minute, 52°C for 1 minute and 68°C for 1 minute, and 1 cycle of 68°C for 7 minutes. Mouse glyceraldehyde-3-phosphate dehydrogenase (GAPDH) was included in the RT-PCR as a loading control with GAPDH-specific primers (5'-CTCAGTGTAGCCCAGGATGC-3' and 5'-ACCACCATGGGAAGGCTGG-3'). The sizes of RT-PCR products for GFAP and GAPDH were 625 bp and 500 bp, respectively.

### *Electrophoretic Mobility Shift Assay*

U373 cells were treated with EGb 761 at a concentration between 0 and 200  $\mu$ g/ml for 3 days and then washed twice to remove EGb 761 before they were lysed in a high-salt buffer containing 20 mmol/L HEPES, pH 7.5, 400 mmol/L KCl, 0.5 mmol/L EDTA, 0.1 mmol/L EGTA, 1 mmol/L dithiothreitol, 20% glycerol, 0.5 mmol/L phenylmethyl sulfonyl fluoride, 2  $\mu$ g/ml each of aprotinin, pepstatin A, leupeptin, and soybean trypsin inhibitor, and 1% Nonidet P-40, on ice for 30 minutes. The cell lysates were centrifuged at 20,000  $\times$  g at 4°C for 5 minutes, and the supernatants were saved as whole cell lysates for the

electrophoretic mobility shift assay. Protein concentration was determined using a DC protein assay kit (Bio-Rad). Oligonucleotides containing respective AP1, AP2, NF- $\kappa$ B, and CREB consensus binding sites were synthesized, annealed, and end-labeled with  $\gamma$ - $^{32}$ P-ATP using T4 polynucleotide kinase, and free  $\gamma$ - $^{32}$ P-ATP was removed by phenol:chloroform extraction and ethanol precipitation.  $^{32}$ P-labeled oligonucleotides of 250,000 cpm were then incubated with 300 ng of protein equivalent whole cell lysates made from each set of EGb 761-treated cells in a volume of 10  $\mu$ l of binding buffer containing 4% glycerol, 1 mmol/L MgCl<sub>2</sub>, 0.5 mmol/L EDTA, 0.5 mmol/L dithiothreitol, 50 mmol/L NaCl, 10 mmol/L Tris-HCl, pH 7.5, and 50  $\mu$ g/ml poly(dI-dC):poly(dI-dC). The mixture was incubated at room temperature for 20 minutes and subjected to 6% native polyacrylamide gel electrophoresis. The gels were dried and exposed to X-ray film. The consensus oligonucleotide sequences were 5'-CGCTT-GATGAGTCAGCCGGAA-3' for AP1, 5'-GATCGAACTGACCGCCCGCGGCCCGT-3' for AP2, 5'-AGTTGAGGGG-ACCTTCCCAGGC-3' for NF- $\kappa$ B, and 5'-AGAGATTGCC-TGACGTCAGAGAGCTAG-3' for CREB.

### Immunofluorescence Staining

Primary murine astrocytes were isolated from 16.5- to 18-day fetuses as described<sup>18,19</sup> and maintained in Dulbecco's modified Eagle's medium supplemented with 10% fetal bovine serum, 50 U/ml penicillin, and 50  $\mu$ g/ml streptomycin in a 37°C, 5% CO<sub>2</sub> incubator. The cells were cultured for 9 to 12 days *in vitro* and then plated in a 24-well plate at a density of  $5 \times 10^4$  cells/well and treated with EGb 761 at indicated concentrations for 3 days. For immunofluorescence staining, the cells were washed with ice-cold PBS at room temperature for 10 minutes and fixed with 4% paraformaldehyde in PBS at room temperature for 30 minutes. After permeabilization with 0.5% Triton X-100 in PBS at room temperature for 30 minutes, the cells were blocked with 0.1% goat serum and 0.5% Triton X-100 in PBS at room temperature for 2 hours. The cells were then incubated with monoclonal anti-GFAP (1:50, Sigma) in blocking solution at 4°C overnight and then with phycoerythrin-conjugated goat anti-mouse-IgG (1:200) in blocking solution at room temperature for 1 hour. Extensive washes with PBS were performed after each step. Omission of the primary antibody in parallel staining was included as a control to ensure no nonspecific staining.

### Nitric Oxide (NO) Production in the Culture Supernatant

Primary astrocytes were prepared as described above. The cells were cultured for 9 to 12 days *in vitro* and then plated in a 24-well plate at a density of  $5 \times 10^4$  cells/well and treated with Dox at 5  $\mu$ g/ml for 3 days. Treatment with the same pH distilled H<sub>2</sub>O was included as a control. Culture supernatants were then collected and spun down briefly to remove cell debris. Cleared supernatants were saved for NO determination, and cells were lysed in RIPA buffer for total protein determination. The NO level in the

supernatants was determined using a Griess assay. Briefly, 50  $\mu$ l of supernatants was mixed with 50  $\mu$ l of 1% sulfanilamide in a 96-well plate and incubated at room temperature for 10 minutes in the dark. Then, 50  $\mu$ l of 0.1% *N*-1-naphthylethylenediamine dihydrochloride was added to the mixture and continued to incubate at room temperature in the dark for additional 10 minutes. Then, the optical absorbance reading was taken at a wavelength of 570 nm and expressed as a fraction of the total cellular protein. A series of sodium nitrite dilutions were included to ensure the readings were in the linear range and to determine absolute NO levels.

### Data Acquisition and Statistical Analysis

Protein and mRNA expression levels were determined using a densitometer, calculated on the basis of the loading controls ( $\beta$ -actin for Western blot and GAPDH for RT-PCR), and expressed as a relative value. Immunohistochemistry and TUNEL-positive cell numbers were obtained using the stereological technique. Briefly, positively stained cells were counted on a systemically random sample of three sections from at least 1 of every 10 saggital sections by three independent individuals, using a view field of  $100 \times 100 \mu$ m (a two-dimensional grid). The cell counting was performed on at least three animals of each group, and three different view fields were chosen randomly within the same micro-anatomical brain regions of each section of the brain. Average values of cell counts were calculated from the pooled data. To ensure the objectivity, all brain sections were blinded for their genetic identity and treatments, and the labels were opened only after the data acquisition was complete. To quantitate GFAP immunoreactivity, digital images of immunostained sections were captured. Photographic and microscopic parameters were kept constant for comparisons. Gray scale-inverted images were generated and analyzed using NIH Image J software as described<sup>26</sup> (also at <http://rsb.info.nih.gov/ij>). Briefly, at least 10 random fields of stained cells and adjacent fields containing no stained cells (background) were selected and assessed for gray values using this software, the differences of gray values between fields containing stained cells and its adjacent background were calculated as a measure of GFAP immunoreactivity. All values expressed as means  $\pm$  SEM. Comparisons among groups were made using two-tailed Student's *t*-test. A *P* value of  $<0.05$  was considered statistically significant (\*), and  $P < 0.001$  highly significant (\*\*).

## Results

### EGb 761 Improves Development and Survival of Tat Transgenic Mice

Tat expression in the brain results in impaired body growth and premature death of Dox-inducible Tat transgenic mice.<sup>17</sup> To investigate whether EGb 761 would have neuroprotective effects on these Tat-induced phenotypes, we first injected mice intraperitoneally with Dox for 7 days and then orally administered EGb 761 for an

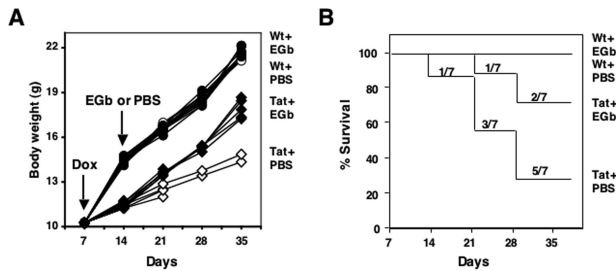


**Figure 1.** Effects of EGb 761 on body growth and survival of Tat transgenic mice. Wild-type and Tat transgenic mice (21 days of age) were injected intraperitoneally with Dox (80 mg/kg/day) for 7 days followed by oral administration of EGb 761 (100 mg/kg/day) for an additional 21 days. EGb 761 was dissolved in PBS, and PBS was included as the vehicle control. Mouse body weight (A) and survival (B) were monitored on a weekly basis. There were seven randomly assigned mice in each group at the beginning of experiments. The body weight was presented for each individual mouse (A), whereas the survival rate was presented for each group (B).

additional 21 days at a dosage of 100 mg/kg/day.<sup>21,27</sup> There were seven age-matched mice in each of four experimental groups (Figure 1, A and B). Mouse survival and growth were monitored on a daily basis. At the beginning of EGb 761 treatment, Tat transgenic mice that had been treated with Dox for 7 days manifested profound and progressive growth retardation, as previously reported,<sup>17</sup> which readily distinguished them from non-transgenic littermate controls (Figure 1A). Seven days of exposure to Dox in these mice led to one death at 14 days, two more deaths by 21 days, two more deaths by 28 days, and the remaining two were cachectic when sacrificed on day 37. In contrast, 7 days exposure of Dox followed by EGb 761 treatment had only one death by 21 days and one additional death by 28 days (Figure 1B), and the survivors in this group showed gains in body weight (from  $12.12 \pm 0.20$  g to  $17.45 \pm 0.65$  g,  $n = 5$ ,  $P < 0.001$ ; Figure 1A). Wild-type C57BL/6 littermate controls exhibited normal growth (from  $14.25 \pm 0.31$  g to  $22.13 \pm 0.49$  g,  $n = 7$ ,  $P < 0.001$ ) and survival during the period of observation (Figure 1, A and B). There was no significant difference in body weight in the wild-type control groups with and without EGb 761 ( $22.13 \pm 0.49$  g versus  $21.68 \pm 0.52$  g,  $n = 7$ ,  $P > 0.05$ ).

### EGb 761 Reduces Astrocytosis and Cell Death in the Brains of Tat Transgenic Mice

To determine histological changes in the brains of Tat transgenic mice in the presence or absence of EGb 761 administration, we harvested tissues at the end of each treatment and performed hematoxylin and eosin (H&E) staining. As we have previously shown,<sup>17</sup> Tat transgenic mice manifested both gross and histological evidence of reactive astrocytosis, inflammation, edema, and brain atrophy in both cerebral cortex (Figure 2A) and hippocampus (Figure 2B). In addition, thinning and disintegration of the granule cell layer in the hippocampus were also evident (Figure 2B). Notably, these pathological changes were much less evident in the brains of Tat transgenic mice treated with EGb 761. We then performed immunohistochemical staining of brain tissues for GFAP, a cellular marker for astrocytosis, and *in situ* apoptosis TUNEL

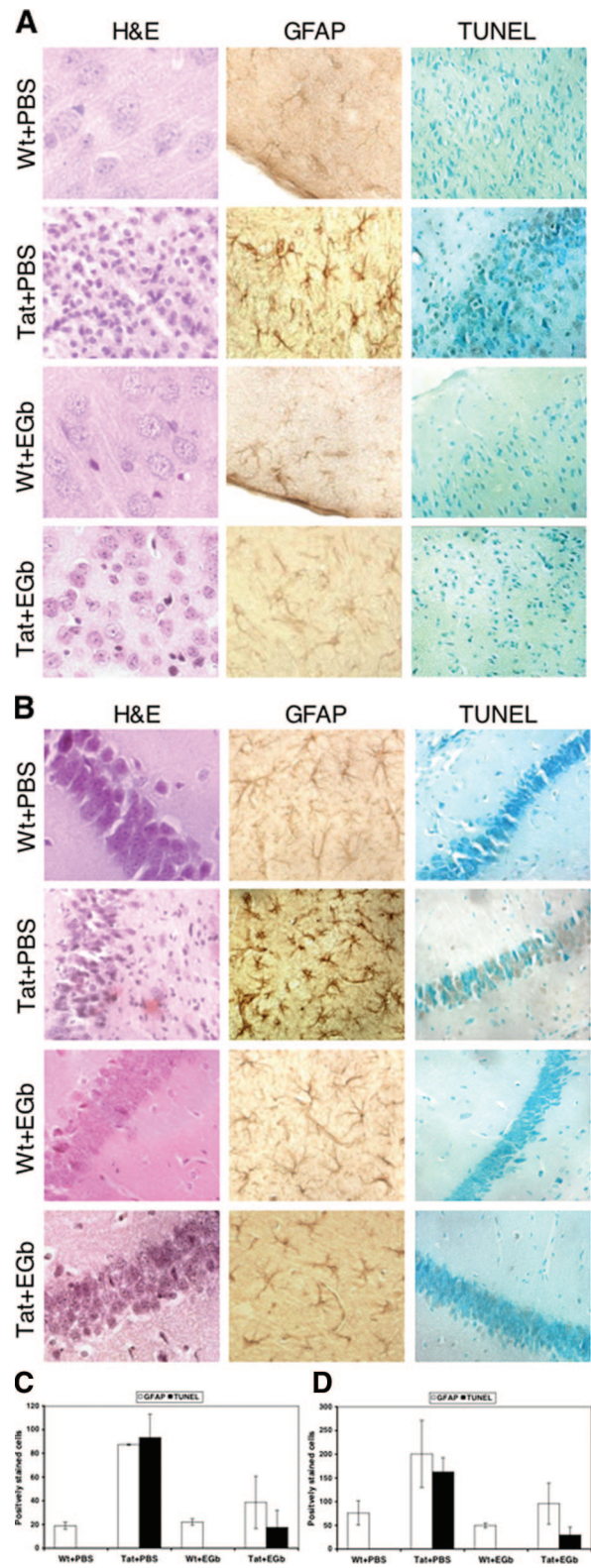


**Figure 2.** Effects of EGb 761 on Tat-induced pathologies. Brain tissues were harvested from mice of each group from Figure 1, fixed in 4% PBS-buffered paraformaldehyde, and embedded in paraffin. Sagittal sections were prepared and stained for H&E, GFAP, and TUNEL. Representative staining of mice in each group was shown for cortex (A) and hippocampus (B), and all sections were scored for GFAP-positive and TUNEL-positive cells separately for cortex (C) and hippocampus (D).

staining for cell death. Consistent with the histological observations, Tat expression markedly increased the number of GFAP-expressing astrocytes in cortex (from  $19.00 \pm 3.00$  to  $87.33 \pm 0.57$ ,  $P < 0.001$ ; Figure 2C) and in hippocampus (from  $76 \pm 25.50$  to  $200.66 \pm 70.43$ ,  $P < 0.01$ ; Figure 2D), whereas EGb 761 administration reduced the number of GFAP-expressing astrocytes in cortex (from  $87.33 \pm 0.57$  to  $38.66 \pm 22.03$ ,  $P < 0.05$ ; Figure 2C) and in hippocampus (from  $200.66 \pm 70.43$  to  $95.57 \pm 43.41$ ,  $P < 0.05$ ; Figure 2D). Similarly, Tat expression markedly increased the number of TUNEL-positive neurons in cortex (from 0 to  $93.25 \pm 19.76$ ,  $P < 0.001$ ; Figure 2C) and in hippocampus (from 0 to  $162.75 \pm 30.28$ ,  $P < 0.001$ ; Figure 2D), whereas EGb 761 administration reduced the number of TUNEL-positive neurons in cortex (from  $93.25 \pm 19.76$  to  $17.50 \pm 14.52$ ,  $P < 0.001$ ; Figure 2C) and in hippocampus (from  $162.75 \pm 30.28$  to  $29.57 \pm 16.74$ ,  $P < 0.001$ ; Figure 2D). These results showed that EGb 761 alleviated HIV-1 Tat protein-induced pathologies including astrocytosis and neuron death.

### Direct Down-Modulation of GFAP Expression by EGb 761

The markedly reduced GFAP expression observed in the brain of EGb 761-treated Tat transgenic mice could result from direct EGb 761 effects on GFAP expression in astrocytes or secondary effects from neuroprotective effects of EGb 761. To test whether EGb 761 would directly affect GFAP expression, we first treated human astrocytoma U373.MG with EGb 761 and then determined GFAP expression at both protein and mRNA levels. Treatment with EGb 761 at concentrations from 0 to 200  $\mu\text{g/ml}$  revealed a dose-dependent reduction of GFAP at the levels of both protein and mRNA (Figure 3A). EGb 761 had no cytotoxic or adverse effects on cell proliferation at

these concentrations, as determined by MTT assay and thymidine incorporation, respectively (data not shown). Similarly, GFAP protein and mRNA were also down-regulated by EGb 761 in Tat-expressing U373.MG cells (U373.Tat) (Figure 3B), which have been shown to express higher levels of GFAP.<sup>19</sup> To determine whether any one of two available purified components of EGb 761, terpene bilobalide (CP160) and ginkgolide B, is responsible for GFAP down-regulation, we treated U373.MG cells with each of them at concentrations corresponding to those in EGb 761. The results showed that CP160 down-regulated GFAP expression at both mRNA and protein levels in a similar manner (Figure 3C). Similar effects were also obtained in Tat-expressing U373.MG cells (Figure 3D). In contrast, ginkgolide B exhibited no detectable effects on GFAP expression (data not shown).

To confirm further the effects of EGb 761 on GFAP expression, we also treated primary murine astrocytes with EGb 761 and performed immunofluorescence staining. Consistent with the results obtained from the astrocytoma cell lines, EGb 761 treatment down-regulated GFAP expression in a dose-dependent manner without detectable effects on cell survival (Figure 4A). Moreover, we also treated wild-type C57BL/6 mice with and without EGb 761 and compared GFAP expression levels between these two groups (Figure 4B). To determine quantitatively the GFAP expression level, we used NIH Image J software and performed the gray-scale analysis of the GFAP staining intensity (Figure 4C). Compared to the PBS control, EGb 761 administration decreased the gray values of GFAP immunoreactivity in cortex (from  $29.77 \pm 16.45$  to  $15.00 \pm 11.45$ ,  $P < 0.05$ ; Figure 4C) and in hippocampus (from  $52.40 \pm 10.26$  to  $6.41 \pm 3.42$ ,  $P < 0.001$ ; Figure 4C). Taken together, these results demonstrated that EGb 761 had direct down-modulatory effects on GFAP gene expression.

### Inhibition of GFAP Gene Transcription by EGb 761

To determine the molecular mechanisms of EGb 761-mediated down-regulated expression of GFAP, we took advantage of a human GFAP promoter-driven firefly luciferase reporter plasmid. We transfected the GFAP-luciferase DNA into U373.MG cells and cultured the cells in the presence of EGb 761 for 2 days. We then harvested these cells for luciferase activity assay. EGb 761 treatment showed a dose-dependent inhibition of GFAP-driven luciferase expression (Figure 5A, open bar), which was in agreement with the RT-PCR results obtained above (Figure 3). These results further confirmed that the EGb 761-mediated down-regulation of GFAP expression occurred at the transcriptional level. Similar results were obtained using primary astrocytes (Figure 5A, closed bar). Genomatix software analysis of the GFAP promoter revealed that four major transcription factors AP1, AP2, NF- $\kappa$ B, and CREB could be major contributors to regulation of GFAP expression in astrocytes. To investigate which transcription factors were directly affected by EGb 761, we measured the binding affinity of these four tran-

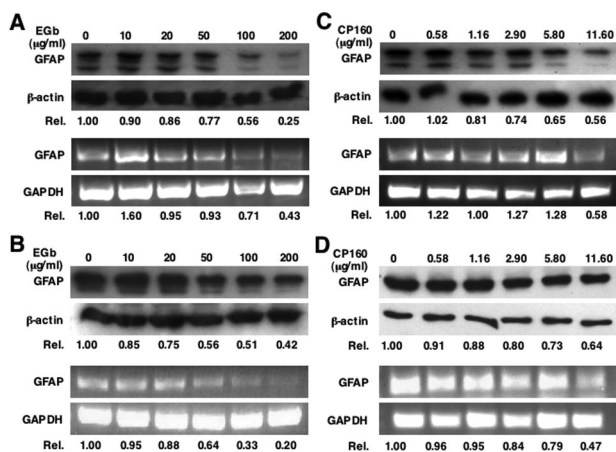


**Figure 3.** Effects of EGb 761 on GFAP expression in astrocytoma cells. Astrocytoma U373 cells (A and C) and its derivative Tat-expressing cells (U373-Tat) (B and D) were treated with EGb 761 (A and B) or CP160 (C and D) at indicated concentrations for 3 days and then harvested for total RNA isolation and cell lysates. GFAP protein and mRNA were determined by Western blot and RT-PCR, respectively.  $\beta$ -Actin and GAPDH were included as controls. GFAP expression was quantitated by a densitometer and expressed in relation to each control (Rel.).

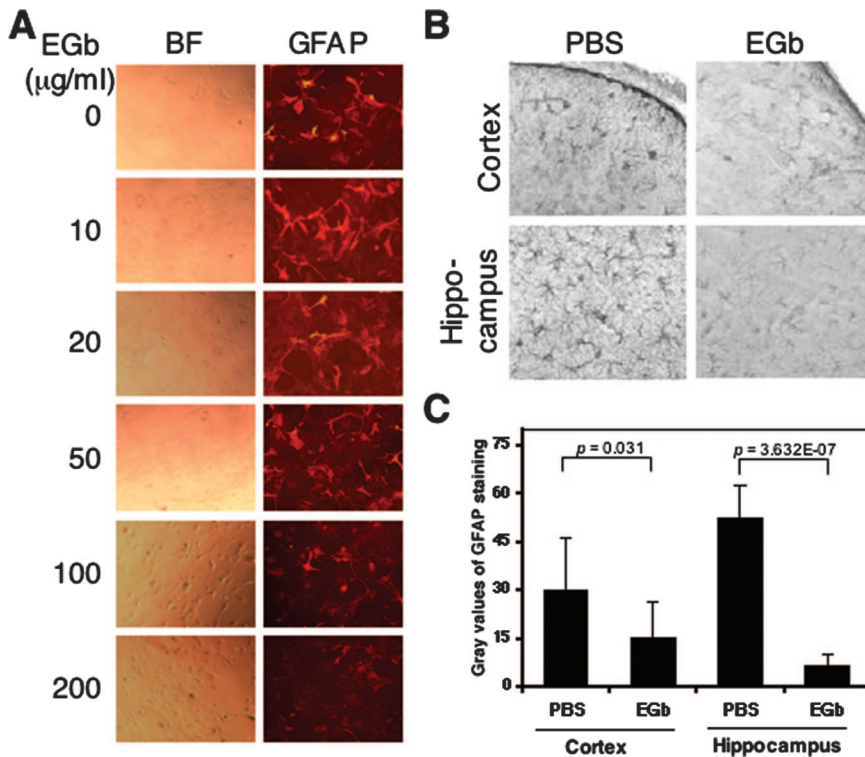


**Figure 4.** Effects of EGb 761 on GFAP expression in primary astrocytes and in the brain. **A:** Primary murine astrocytes were isolated from 16.5-day-old fetuses of wild-type C57BL/6 mice, treated with EGb 761 for 3 days, and immunostained for GFAP expression (right column). The bright field of these cells is shown in the left column (BF), and GFAP staining is shown in the right column (GFAP). Control staining in the absence of anti-GFAP antibody is also included, giving no nonspecific signal (data not shown). **B:** C57BL/6 mice were treated with EGb 761 in PBS (100 mg/kg/day) or vehicle alone for 7 days, and the brain was harvested and processed for immunohistochemical staining for GFAP. The grayscale analysis of GFAP immunoreactivity was performed by a NIH Image J software and is shown in **C**.

scription factors to their cognate consensus DNA-binding sites using an electrophoretic mobility shift assay. We cultured U373.MG cells in the presence of EGb 761 for 3 days and then prepared whole cell lysates from these cells for this assay. EGb 761 treatment at concentrations between 0 and 200 µg/ml decreased the complex formation, shown as closed arrow in Figure 5B, between EGb

761-treated cell lysates and AP1 or NF-κB cognate DNA sequence in a dose-dependent manner but had no detectable effects on the binding of EGb 761-treated cell lysates to AP2 or CREB cognate DNA sequence (Figure 5B). The binding specificity between each transcription factor and its DNA-binding sequence was confirmed by using unlabeled oligonucleotides for competition (data not shown). To further corroborate these findings, we transfected AP1- and NF-κB-dependent luciferase reporter gene plasmids into U373.MG cells, cultured the cells in the presence of EGb 761, and determined the luciferase activity. Similar to the results obtained from the electrophoretic mobility shift assay, EGb 761 treatment inhibited both AP1- and NF-κB-dependent luciferase gene expression in a dose-dependent manner (Figure 5C). These results suggest that EGb 761-mediated down-regulation of GFAP expression is likely attributable to its negative effects on AP1 and NF-κB binding to their respective DNA sites within the GFAP promoter.

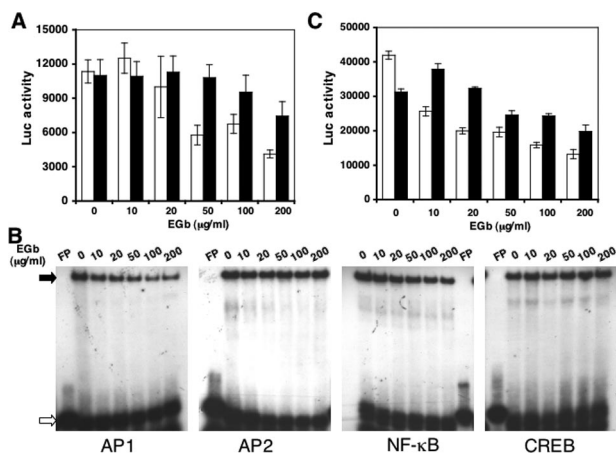


**Figure 5.** Regulation of GFAP transcription by EGb 761. U373 cells (**A**, open bar) and murine primary astrocytes (**A**, closed bar) were transfected with the GFAP promoter-driven luciferase reporter plasmid, or U373 cells were transfected with AP1-dependent luciferase reporter plasmid (**C**, open bar) or NF-κB-dependent luciferase reporter plasmid (**C**, closed bar) using Lipofectamine. Transfected cells were treated with EGb 761 at concentrations as indicated for 2 days, and harvested for luciferase activity assay. Untransfected U373 cells were also treated with EGb 761 at concentrations as indicated for 2 days and harvested for whole cell lysates for electrophoretic mobility shift assay (**B**) in the presence of <sup>32</sup>P-labeled AP1, AP2, NF-κB, and CREB binding site-containing oligonucleotides. **Open arrow:** unbound probe; **closed arrow:** protein-probe complex. FP: free <sup>32</sup>P-labeled probe (no cell lysates added).

### Attenuation of Tat-Induced Neurotoxicity by GFAP Gene Knockout

Tat expression alone is sufficient to up-regulate GFAP expression in astrocytes.<sup>19</sup> The above results showed that EGb 761 was able to directly down-regulate GFAP promoter activity and expression (Figures 3 to 5). Therefore, EGb 761 protection against Tat-induced pathology (Figures 1 and 2) could be attributable to the inhibitory effects of EGb 761 on the GFAP promoter and subsequent decreased levels of GFAP protein. To determine the role of GFAP expression in Tat-induced pathologies, we bred GFAP-null mice with Tat transgenic mice (Tat) to

**Table 1.** Experimental Groups and the Number of Animals

Treatment/ genotype	dW*	Dox*	Dox + PBS†	Dox + EGb†
Wt	3	6	4	6
Tat	3	8	5	6
GFAP-null	3	6	6	7
GFAP-null/Tat	6	6	6	6

\*Animals were treated with dW or Dox (80 mg/kg/day) for 7 days.

†Animals were treated with Dox (80 mg/kg/day) for 7 days, followed by PBS or EGb 761 (100 mg/kg/day) for an additional 7 days.

obtain GFAP-null/Tat mice. We then randomly divided the mice into four groups for four treatment regimens: distilled water only (dW), Dox only, Dox followed by PBS (Dox + PBS), and Dox followed by EGb 761 (Dox + EGb). As controls, we included wild-type C57BL/6 (Wt), Tat, and GFAP-null mice in these experiments (Table 1). Body weight was monitored on a daily basis during the entire period of treatment. Both Wt and GFAP-null mice displayed no significant differences in body weight between dW treatment and Dox treatment, and there were also no significant differences in body weight between Dox + PBS and Dox + EGb (Figure 6A). As shown previously (Figure 1A), Tat mice given Dox treatment showed significantly less weight gain than those given dW as a control ( $0.275 \pm 0.528$  g versus  $4.19 \pm 0.33$  g,  $P < 0.001$ ; Figure 6A). However, Tat mice given continued treatment with EGb 761 had significantly higher weight gain than those given PBS as a control ( $6.21 \pm 1.01$  versus  $2.23 \pm 1.23$ ,  $P < 0.001$ ). Moreover, the weight gain of Tat mice treated with Dox + EGb appeared to be similar to Wt ( $6.21 \pm 1.01$  versus  $7.03 \pm 1.70$ ,  $P > 0.05$ ), GFAP-null ( $6.21 \pm 1.01$  versus  $6.21 \pm 0.56$ ,  $P > 0.05$ ), and GFAP-null/Tat mice ( $6.21 \pm 1.01$

versus  $6.04 \pm 1.04$ ,  $P > 0.05$ ). In contrast, GFAP-null/Tat mice also had less weight gain in Dox treatment than dW control ( $1.56 \pm 0.24$  versus  $3.90 \pm 1.04$ ,  $P < 0.05$ ), but it was significantly higher than Tat mice treated with Dox ( $1.56 \pm 0.24$  versus  $0.275 \pm 0.528$ ,  $P < 0.001$ ). Moreover, GFAP-null/Tat mice treated with Dox followed by PBS gained more weight than Tat mice with the same treatment regimen ( $4.54 \pm 1.09$  versus  $2.23 \pm 1.23$ ,  $P < 0.001$ ). More importantly, there did not appear to be a significant difference in weight gain between GFAP-null/Tat mice treated with Dox + PBS and those given Dox + EGb ( $4.53 \pm 1.09$  versus  $6.04 \pm 1.04$ ,  $P > 0.05$ ). In addition, we also harvested brain tissues at the end of each treatment regimen and processed them for H&E, Iba-1, CD3, MAP-2, S100 $\beta$ , and TUNEL staining. In hippocampus, Dox treatment of Tat mice resulted in thinning and disintegration of the granule cell layer but had no effect in Wt, GFAP-null, and GFAP-null/Tat mice (Figure 7). Tat mice treated with Dox + EGb showed significant restoration of the granule cell layer structure (Figure 7). Iba-1 staining showed that there were significant increases in the number of Iba-1-positive cells in Tat mice treated with Dox and Dox + PBS compared to all others (Figure 6B). Moreover, Iba-1-positive cells in these two groups exhibited more intense staining and morphological transformation from a ramified to an amoeboid phenotype (Supplemental Figure 1A, see <http://ajp.amjpathol.org>), both of which are typical characteristics of activated macrophages/microglia. Furthermore, either EGb 761 treatment or GFAP knockout (GFAP-null) considerably inhibited activation of macrophages/microglia induced by Tat expression, ie, decrease in the number of Iba-1-positive cells (Figure 6B) and the staining intensity and morphological change to the ramified phenotype (Supplemental Figure 1A, see <http://ajp.amjpathol.org>). Similarly, the CD3 staining showed that Tat expression led to perivascular accumulation and infiltration of T lymphocytes in Tat mice treated with Dox and Dox + PBS, whereas there were very few CD3-positive cells in all others (Supplemental Figure 1, see <http://ajp.amjpathol.org>). The results also showed that there was a significant decrease of CD3-positive cells in EGb 761-treated mice and GFAP knockout (GFAP-null) mice.

As shown previously,<sup>17</sup> Dox treatment induced neuron loss in the brains of Tat mice compared to dW treatment ( $49.32 \pm 8.33$  versus  $83.60 \pm 5.77$ ,  $P < 0.001$ ; Figure 8A), as determined by MAP-2 staining (Supplemental Figure 1C, see <http://ajp.amjpathol.org>). The number of MAP-2-positive neurons in Tat mice treated with Dox + PBS was even lower than Tat mice treated with Dox alone ( $38.73 \pm 9.28$  versus  $83.60 \pm 5.77$ ,  $P < 0.001$ ; Figure 8A), suggesting that there were still secondary effects from Tat expression even when Tat expression was discontinued in these mice. However, compared to Dox + PBS treatment, Dox + EGb treatment resulted in a significantly higher number of MAP-2-positive neurons in the brain of Tat mice ( $88.00 \pm 25.36$  versus  $38.73 \pm 9.28$ ,  $P < 0.001$ ; Figure 8A). Meanwhile, Wt, GFAP-null, and GFAP-null/Tat mice showed no significant differences in the number of MAP-2-positive neurons among different treatments. Similarly, Dox treatment induced neuron ap-

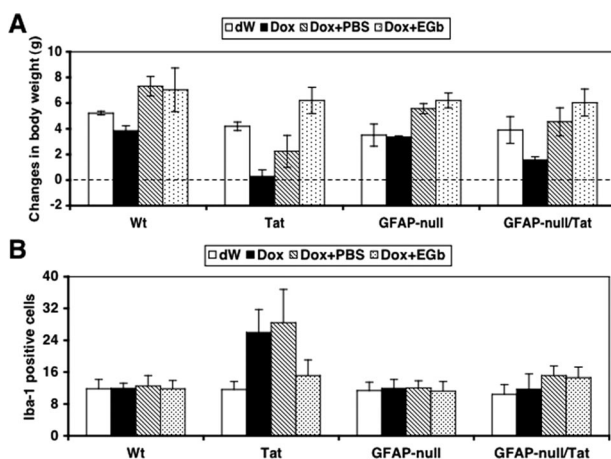


**Figure 6.** Effects of GFAP gene knockout on development of Tat transgenic mice and activation of macrophages/microglia. Twenty-one-day-old mice of C57BL/6 wild-type (Wt), Tat transgenic (Tat), GFAP-null, and GFAP-null/Tat transgenic (GFAP-null/Tat) were treated with Dox only for 7 days (80 mg/kg/day) (Dox), distilled water for 7 days (dW), Dox for 7 days followed by EGb 761 (100 mg/kg/day) for 7 days (Dox + EGb), or Dox for 7 days followed by PBS for 7 days (Dox + PBS). **A:** Body weight was monitored on a daily basis and calculated for net weight changes at the end of each treatment. At the end of each treatment, mouse brains were harvested and processed for immunohistochemistry staining for Iba-1-positive cells. **B:** The cell counting was performed within the hippocampal region of the brain using stereology.



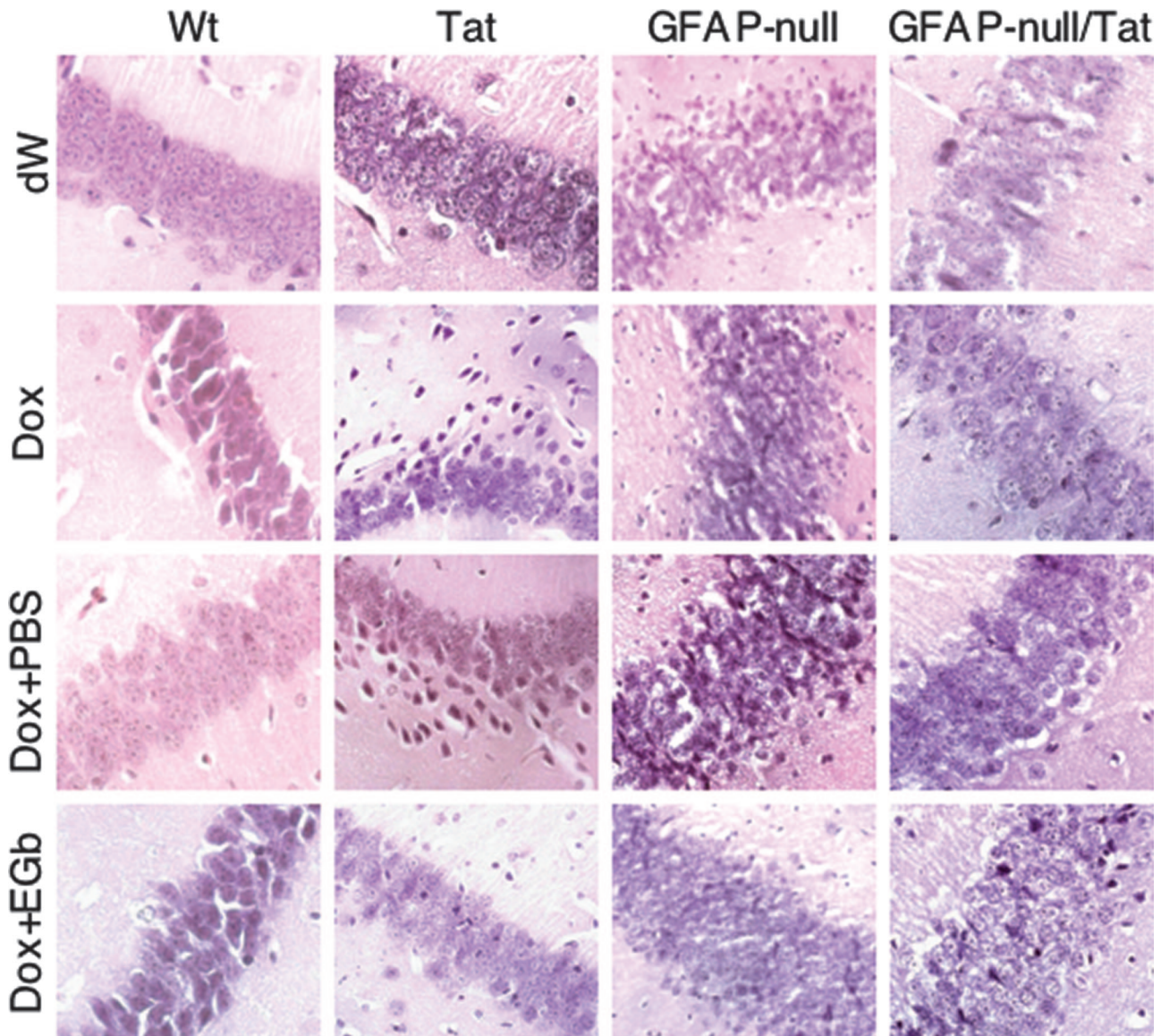


**Figure 7.** Effects of GFAP gene knockout on hippocampal morphology of Tat transgenic mice. At the end of each treatment described in Figure 6, mouse brains were harvested and processed for H&E staining. Representative images were taken in the hippocampal region of the brain.

optosis in the brains of Tat mice compared to dW treatment ( $80.36 \pm 32.80$  versus  $3.4 \pm 5.63$ ,  $P < 0.001$ ; Figure 8B), as determined by TUNEL staining (Supplemental Figure 1D, see <http://ajp.amjpathol.org>). In agreement with the MAP-2 staining results, the number of TUNEL-positive neurons in Tat mice treated with Dox + PBS was much higher than dW treatment ( $162.75 \pm 30.28$  versus  $3.4 \pm 5.63$ ,  $P < 0.001$ ; Figure 8B). Compared to Dox + PBS treatment, Dox + EGb treatment resulted in a significantly lower number of TUNEL-positive neurons in the brain of Tat mice ( $29.57 \pm 16.74$  versus  $162.75 \pm 30.28$ ,  $P < 0.001$ ; Figure 8B). In contrast, little apoptosis was detected in the brains of Wt, GFAP-null, and GFAP-null/Tat mice under different treatment regimens. All these observed pathological differences were not likely attributable to the differences in the number of astrocytes in the brains of these four types of mice. As expected, we indeed only detected a slightly increase of the number of

S100 $\beta$ -positive cells in the brain of Tat mice treated with Dox and Dox + PBS but little differences in other mice with different treatments (data not shown). Also, the improvement in these pathological phenotypes in GFAP-null/Tat mice was not attributable to a decrease in Tat expression because the results showed that Tat expression in these mice was even higher than Tat transgenic mice (Figure 9A) and a higher Tat-expressing transgenic line Tg 271 was used to generate these GFAP-null/Tat transgenic mice.

One of the proposed mechanisms for EGb 761 neuroprotective function is its anti-oxidative activity,<sup>28</sup> and Tat has been shown to alter the intracellular redox level.<sup>29–32</sup> Thus, we next determined effects of Tat expression on nitric oxide (NO) production in Tat transgenic mice using primary astrocytes. We prepared astrocyte cultures from wild-type and Tat transgenic mice and treated them with Dox. We then collected the supernatants and measured

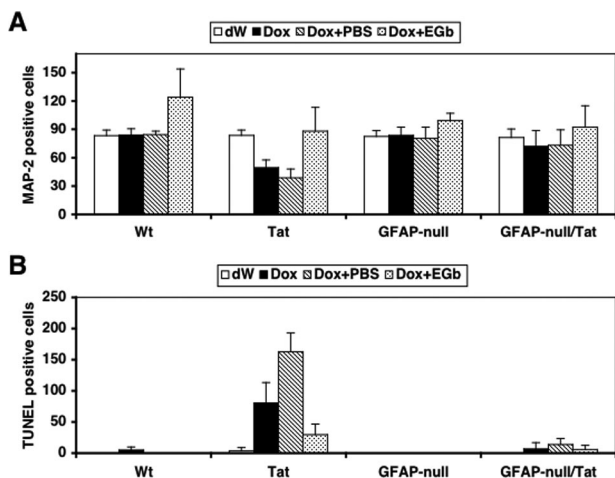


**Figure 8.** Effects of GFAP gene knockout on neuron survival and apoptosis in hippocampus of Tat transgenic mice. At the end of each treatment described in Figure 6, mouse brains were harvested and processed for MAP-2 (A) or TUNEL staining (B). The cell counting was performed within the hippocampal region of the brain using stereology.

the NO levels in these supernatants. The results confirmed that Tat expression in this model also led to increased NO production (Figure 9B) and, as a result, alteration of intracellular redox status.

## Discussion

### Neurotherapeutic Function of EGb 761 against Tat Neurotoxicity

Neuroprotective functions of EGb 761 have been demonstrated in experimental models and clinical studies of

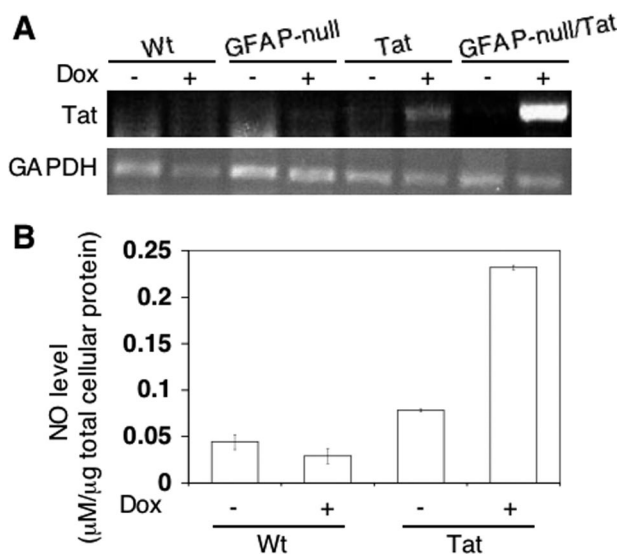


**Figure 9.** Tat expression in the brain of GFAP-null/Tat mice and its effects on NO production. Total RNA was isolated from wild-type (Wt), GFAP knockout (GFAP-null), Tat transgenic (Tat), and GFAP knockout/Tat transgenic (GFAP-null/Tat) mice treated with (+) and without (-) Dox and assayed for Tat mRNA level by RT-PCR. A: RT-PCR for GAPDH was included as a control. B: For NO experiments, primary astrocytes were prepared and exposed to Dox (5 μg/ml) for 3 days, and the culture supernatants were collected to determine NO production using a Griess assay. Distilled H<sub>2</sub>O with the same pH was used as the control (-). The NO levels were normalized to the total amount of the cellular protein.

neurological diseases including dementia. This study demonstrated that EGb 761 had neurotherapeutic effects against HIV-1 Tat-induced neuropathologies in the transgenic mouse model. EGb 761 administration after Dox treatment improved development and survival of Tat transgenic mice (Figures 1 and 6A). Consistent with these findings, astrocytosis was markedly reduced based on the number of GFAP-positive astrocytes (Figure 2) and the level of GFAP expression (Figure 4C), and apoptosis was reduced as well (Figures 2 and 8B). The mechanisms of EGb 761 neuroprotective effects are believed to be mediated via several of its properties, including roles as an antioxidant, a free-radical scavenger, a membrane stabilizer, and an inhibitor of platelet-activating factor (PAF).<sup>33,34</sup> The flavonoids, the major component of EGb 761, have been shown to be neuroprotective through their potent antioxidant activity.<sup>29</sup> Alteration of intracellular redox has long been linked to HIV-associated dementia and/or Tat neurotoxicity.<sup>35,36</sup> Thus, EGb 761 neuroprotective function against Tat neurotoxicity, at least in part, is mediated by neutralizing Tat-induced oxidative stress (Figure 9B). EGb 761 also has anti-inflammatory effects and protective actions against brain damage through its terpenes and ginkgolides.<sup>37,38</sup> The ginkgolide B acts as an antagonist of PAF,<sup>37</sup> a factor that induces proinflammatory effects<sup>39</sup> and is activated in the HIV-infected brain.<sup>40</sup> Besides the free radical theory, inflammation is noted in the brains of HIV-infected individuals and of Tat transgenic mice.<sup>17,41</sup> When we treated mice with terpene bilobalide and ginkgolide B at equivalent composition percentages as those present in EGb 761, only terpene bilobalide produced neuroprotective effects (Figure 3, C and D; data not shown). Interestingly, our results showed that EGb 761 treatment also greatly alleviated inflammatory response induced by Tat expression, ie, reduced central nervous system infiltration of T lymphocytes and macrophage/microglia activation (Figure 6B; and Supplemental Figure 1, A and B, see <http://ajp.amjpathol.org>). Several studies have shown that flavonoids of EGb 761 inhibit HIV-1 entry and replication.<sup>42-44</sup> Taken together, all these studies raise the possibility of using EGb 761 as an alternative medication for treating HIV-induced neurological disorders. These results also confirm that inflammation and free radical production are likely the main events leading to Tat neurotoxicity and HIV-associated neuropathologies.

### Regulation of GFAP Expression in Astrocytes by EGb 761

GFAP is a type-III intermediate filament and was first identified in astrocytes.<sup>45</sup> The gene is highly conserved throughout vertebrate evolution, suggesting that it plays a critical function in the central nervous system. GFAP protein expression is developmentally regulated and is up-regulated during the astrocytosis that occurs in response to most brain injuries.<sup>46</sup> These changes in protein levels are controlled primarily through transcriptional regulation.<sup>47,48</sup> EGb 761 has been shown to alter expression of a number of host genes.<sup>49</sup> Recent cDNA microarray stud-

ies have revealed that EGB 761 modified the expression of genes encoding growth factors, signaling and structural proteins, transcription factors, and metabolic enzymes.<sup>50,51</sup> Our results showed that EGB 761 directly down-regulated GFAP expression at both protein and mRNA levels, and in astrocytoma cells, primary astrocytes *in vitro*, and *in vivo* (Figures 3 and 4). These findings are of interest because previous studies of EGB 761 effects on GFAP immunoreactivity in astrocytes after brain injury have been inconsistent. For instance, one group found little change in GFAP expression in astrocytes exposed to EGB 761,<sup>52</sup> whereas a more recent study found inhibitory effects of EGB 761 on GFAP expression.<sup>53</sup> The discrepancy between these studies may be related to the dosage and the exposure time of EGB 761. We further found that GFAP down-regulation by EGB 761 occurred at the transcriptional level, using the GFAP promoter-driven reporter gene assay (Figure 5A) and that the down-regulation was likely attributable to negative effects of EGB 761 on the activity of the transcription factors AP1 and NF- $\kappa$ B (Figure 5, B and C). Consistent with the antioxidant activity of EGB 761, AP1 and NF- $\kappa$ B activities are known to be regulated by intracellular redox levels.<sup>54,55</sup> Moreover, inhibition of astroglial NF- $\kappa$ B activity has been associated with reduced inflammation and improved functional recovery after spinal cord injury,<sup>56</sup> whereas AP1 up-regulation is often noted in activated astrocytes.<sup>46</sup> Because both AP1 and NF- $\kappa$ B are important regulators for expression of many cytokines and chemokines, it is conceivable that reduced activities of these transcription factors by EGB 761 and resulting decreased infiltration of inflammatory cells into the brain contribute to the protective function of EGB 761 against Tat neurotoxicity.

### *Direct Involvement of GFAP Activation in Tat Neurotoxicity*

Tat expression alone is sufficient to up-regulate GFAP expression in astrocytes *in vitro* and *in vivo*.<sup>17,19</sup> Thus, the finding that EGB 761 directly down-regulated GFAP transcription prompted us to determine whether GFAP was integral to Tat neurotoxicity. To our surprise, Tat expression in the brains of GFAP-null mice led to much less developmental retardation, inflammation, astrocytosis, and neuron apoptosis, and the effects of genetic deletion of GFAP expression on Tat neurotoxicity were similar to those of EGB 761 treatment (Figures 6 to 8). These findings suggest that GFAP up-regulation is directly involved in Tat neurotoxicity, even though EGB 761 protective functions against Tat neurotoxicity could also reflect reduced Tat expression in the brain of inducible Tat transgenic mice.<sup>17</sup> GFAP overexpression in GFAP transgenic mice has been found to form cytoplasmic aggregates of intermediate filaments that are identical to Rosenthal fibers, the hallmark feature of Alexander disease and impaired development and premature death.<sup>57</sup> A recent microarray gene expression analysis on brains from these GFAP overexpressing transgenics has revealed that marked elevation of GFAP results in changes of gene expression relating to stress responses, immune activa-

tion, and neuron survival.<sup>58</sup> Our recent studies have shown that Tat expression in astrocytes also directly affects neuronal survival.<sup>19</sup> Whether any of these genes are involved in GFAP-mediated Tat neurotoxicity remains to be determined. Moreover, serum or cerebrospinal fluid GFAP has long been explored as a biomarker for a number of neurological diseases including stroke and multiple sclerosis.<sup>59,60</sup> Thus, GFAP could represent a new and reliable biomarker for progression and treatment of HIV-associated neuropathogenesis.

### *Astrocytosis as an Auxiliary Perpetrator for Neurodegenerative Diseases*

In higher vertebrates, astrocytes make up a substantial proportion of the central nervous system. Under normal conditions astrocytes are involved in maintenance of the extracellular ionic environment and pH, uptake of extracellular glutamate, maintenance of the blood-brain barrier, and supply of neurons with metabolic substrates.<sup>61</sup> After injury, either as a result of trauma, disease, genetic disorders, or chemical insult, astrocytes become reactive and respond in a typical manner, termed astrocytosis.<sup>62</sup> Astrocytosis is characterized by rapid synthesis of GFAP and is demonstrated by an increase in the protein level or by immunostaining with GFAP antibody. Depending on the *in vivo* insult, astrocytosis may either reduce or exacerbate damage to neural tissue. Reactive astrocytes repair damaged neural tissues through release of neurotrophic factor and antioxidants and degradation of extracellular deposits.<sup>63</sup> In contrast, release of reactive oxygen species, cytokines, nitric oxide, and proteases by reactive astrocytes can contribute to neurodegeneration.<sup>64–66</sup> Identification of GFAP as a mediator of Tat neurotoxicity in our present study supports the notion that astrocytosis indeed provokes Tat neurotoxicity and HIV-associated neuropathogenesis.

In conclusion, we report that EGB 761 has therapeutic activity against Tat neurotoxicity. The anti-oxidant and anti-inflammatory activities of EGB 761 may account for its down-regulatory effects on GFAP expression, and the protective functions of EGB 761 against Tat protein-induced neurotoxicity.

### *Acknowledgments*

We thank the Ipsen Institute, France, and Dr. Yves Christen for generously providing EGB 761 and purified terpene bilobalide and ginkgolide B; Dr. Michael Brenner for providing the human GFAP promoter-driven luciferase reporter plasmid; and Dr. Janice Blum, Dr. Ghalib Alkhatib, and Dr. Chao-Hung Lee for advice.

### *References*

1. Price RW, Brew B, Sidtis J, Rosenblum M, Scheck AC, Cleary P: The brain in AIDS: central nervous system HIV-1 infection and AIDS dementia complex. *Science* 1988, 239:586–592
2. Brew BJ, Rosenblum M, Cronin K, Price RW: AIDS dementia complex

- and HIV-1 brain infection: clinical-virological correlations. *Ann Neurol* 1995, 38:563–570
3. Glass JD, Fedor H, Wesselingh SL, McArthur JC: Immunocytochemical quantitation of human immunodeficiency virus in the brain: correlation with dementia. *Ann Neurol* 1995, 38:755–762
  4. Nath AGJ, Mattson MP, Magnuson DSK, Jones M, Berger JR: Role of viral proteins in HIV-1 neuropathogenesis with emphasis on Tat. *NeuroAIDS* 1998, 1
  5. McArthur JC, Haughey N, Gartner S, Conant K, Pardo C, Nath A, Sacktor N: Human immunodeficiency virus-associated dementia: an evolving disease. *J Neurovirol* 2003, 9:205–221
  6. Sacktor N, McDermott MP, Marder K, Schifitto G, Selnes OA, McArthur JC, Stern Y, Albert S, Palumbo D, Kieburtz K, De Marcaida JA, Cohen B, Epstein L: HIV-associated cognitive impairment before and after the advent of combination therapy. *J Neurovirol* 2002, 8:136–142
  7. Oberpichler H, Beck T, Abdel-Rahman MM, Bielenberg GW, Kriegstein J: Effects of Ginkgo biloba constituents related to protection against brain damage caused by hypoxia. *Pharmacol Res Commun* 1988, 20:349–368
  8. Szabo ME, Droy-Lefaix MT, Doly M: Direct measurement of free radicals in ischemic/reperfused diabetic rat retina. *Clin Neurosci* 1997, 4:240–245
  9. Kleijnen J, Knipschild P: Ginkgo biloba for cerebral insufficiency. *Br J Clin Pharmacol* 1992, 34:352–358
  10. Rai GS, Shovlin C, Wesnes KA: A double-blind, placebo controlled study of Ginkgo biloba extract ('tanakan') in elderly outpatients with mild to moderate memory impairment. *Curr Med Res Opin* 1991, 12:350–355
  11. Le Bars PL, Katz MM, Berman N, Itil TM, Freedman AM, Schatzberg AF: A placebo-controlled, double-blind, randomized trial of an extract of Ginkgo biloba for dementia. North American EGb Study Group. *JAMA* 1997, 278:1327–1332
  12. Oken BS, Storzbach DM, Kaye JA: The efficacy of Ginkgo biloba on cognitive function in Alzheimer disease. *Arch Neurol* 1998, 55:1409–1415
  13. Blumenthal M (Ed): *The Complete German Commission E Monographs: Therapeutic Guides to Herbal Medicines*. Austin, American Botanical Council, 1998
  14. Christen Y: Oxidative stress and Alzheimer disease. *Am J Clin Nutr* 2000, 71:621S–629S
  15. Yao Z, Drieu K, Papadopoulos V: The Ginkgo biloba extract EGb 761 rescues the PC12 neuronal cells from beta-amyloid-induced cell death by inhibiting the formation of beta-amyloid-derived diffusible neurotoxic ligands. *Brain Res* 2001, 889:181–190
  16. Liu Y, Jones M, Hingtgen CM, Bu G, Larabee N, Tanzi RE, Moir RD, Nath A, He JJ: Uptake of HIV-1 tat protein mediated by low-density lipoprotein receptor-related protein disrupts the neuronal metabolic balance of the receptor ligands. *Nat Med* 2000, 6:1380–1387
  17. Kim BO, Liu Y, Ruan Y, Xu ZC, Schantz L, He JJ: Neuropathologies in transgenic mice expressing human immunodeficiency virus type 1 Tat protein under the regulation of the astrocyte-specific glial fibrillary acidic protein promoter and doxycycline. *Am J Pathol* 2003, 162:1693–1707
  18. Zhou BY, He JJ: Proliferation inhibition of astrocytes, neurons, and non-glial cells by HIV-1 Tat protein. *Neurosci Lett* 2004, 359:155–158
  19. Zhou BY, Liu Y, Kim B, Xiao Y, He JJ: Astrocyte activation and dysfunction and neuron death by HIV-1 Tat expression in astrocytes. *Mol Cell Neurosci* 2004, 27:296–305
  20. Guidetti C, Paracchini S, Lucchini S, Cambieri M, Marzatico F: Prevention of neuronal cell damage induced by oxidative stress in-vitro: effect of different Ginkgo biloba extracts. *J Pharm Pharmacol* 2001, 53:387–392
  21. Bastianetto S, Ramassamy C, Dore S, Christen Y, Poirier J, Quirion R: The Ginkgo biloba extract (EGb 761) protects hippocampal neurons against cell death induced by beta-amyloid. *Eur J Neurosci* 2000, 12:1882–1890
  22. Drieu K: Preparation and definition of Ginkgo biloba extract. *Presse Med* 1986, 15:1455–1457
  23. Segovia J, Vergara P, Brenner M: Differentiation-dependent expression of transgenes in engineered astrocyte cell lines. *Neurosci Lett* 1998, 242:172–176
  24. McCall MA, Gregg RG, Behringer RR, Brenner M, Delaney CL, Galbreath EJ, Zhang CL, Pearce RA, Chiu SY, Messing A: Targeted deletion in astrocyte intermediate filament (Gfap) alters neuronal physiology. *Proc Natl Acad Sci USA* 1996, 93:6361–6366
  25. Ferrante RJ, Klein AM, Dedeeoglu A, Beal MF: Therapeutic efficacy of EGb761 (Ginkgo biloba extract) in a transgenic mouse model of amyotrophic lateral sclerosis. *J Mol Neurosci* 2001, 17:89–96
  26. Abramoff MD, Magelhaes PJ, Ram SJ: Image processing with ImageJ. *Biophotonics Int* 2004, 11:36–42
  27. Wu WR, Zhu XZ: Involvement of monoamine oxidase inhibition in neuroprotective and neurorestorative effects of Ginkgo biloba extract against MPTP-induced nigrostriatal dopaminergic toxicity in C57 mice. *Life Sci* 1999, 65:157–164
  28. Christen Y: Ginkgo biloba and neurodegenerative disorders. *Front Biosci* 2004, 9:3091–3104
  29. Ehret A, Westendorp MO, Herr I, Debatin KM, Heeney JL, Frank R, Krammer PH: Resistance of chimpanzee T cells to human immunodeficiency virus type 1 Tat-enhanced oxidative stress and apoptosis. *J Virol* 1996, 70:6502–6507
  30. Opalenik SR, Ding Q, Mallery SR, Thompson JA: Glutathione depletion associated with the HIV-1 TAT protein mediates the extracellular appearance of acidic fibroblast growth factor. *Arch Biochem Biophys* 1998, 351:17–26
  31. Toborek M, Lee YW, Pu H, Malecki A, Flora G, Garrido R, Hennig B, Bauer HC, Nath A: HIV-Tat protein induces oxidative and inflammatory pathways in brain endothelium. *J Neurochem* 2003, 84:169–179
  32. Liu X, Jana M, Dasgupta S, Koka S, He J, Wood C, Pahan K: Human immunodeficiency virus type 1 (HIV-1) tat induces nitric-oxide synthase in human astroglia. *J Biol Chem* 2002, 277:39312–39319
  33. Kobuchi H, Droy-Lefaix MT, Christen Y, Packer L: Ginkgo biloba extract (EGb 761): inhibitory effect on nitric oxide production in the macrophage cell line RAW 264.7. *Biochem Pharmacol* 1997, 53:897–903
  34. Yan LJ, Droy-Lefaix MT, Packer L: Ginkgo biloba extract (EGb 761) protects human low density lipoproteins against oxidative modification mediated by copper. *Biochem Biophys Res Commun* 1995, 212:360–366
  35. Sacktor N, Haughey N, Cutler R, Tamara A, Turchan J, Pardo C, Vargas D, Nath A: Novel markers of oxidative stress in actively progressive HIV dementia. *J Neuroimmunol* 2004, 157:176–184
  36. Lipton SA: Neuronal injury associated with HIV-1 and potential treatment with calcium-channel and NMDA antagonists. *Dev Neurosci* 1994, 16:145–151
  37. Panetta T, Marcheselli VL, Braquet P, Spinnewyn B, Bazan NG: Effects of a platelet activating factor antagonist (BN 52021) on free fatty acids, diacylglycerols, polyphosphoinositides and blood flow in the gerbil brain: inhibition of ischemia-reperfusion induced cerebral injury. *Biochem Biophys Res Commun* 1987, 149:580–587
  38. Oberpichler H, Sauer D, Rossberg C, Mennel HD, Kriegstein J: PAF antagonist ginkgolide B reduces postischemic neuronal damage in rat brain hippocampus. *J Cereb Blood Flow Metab* 1990, 10:133–135
  39. McGeer PL, McGeer EG: The inflammatory response system of brain: implications for therapy of Alzheimer and other neurodegenerative diseases. *Brain Res Brain Res Rev* 1995, 21:195–218
  40. Perry SW, Hamilton JA, Tjoelker LW, Dbaibo G, Dzenko KA, Epstein LG, Hannun Y, Whittaker JS, Dewhurst S, Gelbard HA: Platelet-activating factor receptor activation. An initiator step in HIV-1 neuropathogenesis. *J Biol Chem* 1998, 273:17660–17664
  41. Merrill JE, Chen IS: HIV-1, macrophages, glial cells, and cytokines in AIDS nervous system disease. *FASEB J* 1991, 5:2391–2397
  42. Kitamura K, Honda M, Yoshizaki H, Yamamoto S, Nakane H, Fukushima M, Ono K, Tokunaga T: Baicalin, an inhibitor of HIV-1 production in vitro. *Antiviral Res* 1998, 37:131–140
  43. Chao SH, Fujinaga K, Marion JE, Taube R, Sausville EA, Senderowicz AM, Peterlin BM, Price DH: Flavopiridol inhibits P-TEFb and blocks HIV-1 replication. *J Biol Chem* 2000, 275:28345–28348
  44. Li BQ, Fu T, Dongyan Y, Mikovits JA, Ruscetti FW, Wang JM: Flavonoid baicalin inhibits HIV-1 infection at the level of viral entry. *Biochem Biophys Res Commun* 2000, 276:534–538
  45. Eng LF: Glial fibrillary acidic protein (GFAP): the major protein of glial intermediate filaments in differentiated astrocytes. *J Neuroimmunol* 1985, 8:203–214
  46. Eddleston M, Mucke L: Molecular profile of reactive astrocytes—implications for their role in neurologic disease. *Neuroscience* 1993, 54:15–36

47. Sarthy PV, Fu M: Transcriptional activation of an intermediate filament protein gene in mice with retinal dystrophy. *DNA* 1989, 8:437–446
48. Landry CF, Ivy GO, Brown IR: Developmental expression of glial fibrillary acidic protein mRNA in the rat brain analyzed by in situ hybridization. *J Neurosci Res* 1990, 25:194–203
49. DeFeudis F: Effects of Ginkgo biloba extract (EGb 761) on gene expression: possible relevance to neurological disorders and age-associated cognitive impairment. *Drug Dev Res* 2002, 57:214–235
50. Watanabe CM, Wolfram S, Ader P, Rimbach G, Packer L, Maguire JJ, Schultz PG, Gohil K: The in vivo neuromodulatory effects of the herbal medicine ginkgo biloba. *Proc Natl Acad Sci USA* 2001, 98:6577–6580
51. Li W, Trovero F, Cordier J, Wang Y, Drieu K, Papadopoulos V: Prenatal exposure of rats to Ginkgo biloba extract (EGb 761) increases neuronal survival/growth and alters gene expression in the developing fetal hippocampus. *Brain Res Dev Brain Res* 2003, 144:169–180
52. Attella MJ, Hoffman SW, Stasio MJ, Stein DG: Ginkgo biloba extract facilitates recovery from penetrating brain injury in adult male rats. *Exp Neurol* 1989, 105:62–71
53. Brailowsky S, Montiel T: Motor function in young and aged hemiplegic rats: effects of a Ginkgo biloba extract. *Neurobiol Aging* 1997, 18:219–227
54. Zwacka RM, Zhou W, Zhang Y, Darby CJ, Dudus L, Halldorson J, Oberley L, Engelhardt JF: Redox gene therapy for ischemia/reperfusion injury of the liver reduces AP1 and NF-kappaB activation. *Nat Med* 1998, 4:698–704
55. Pladzyk A, Reddy AB, Yadav UC, Tammali R, Ramana KV, Srivastava SK: Inhibition of aldose reductase prevents lipopolysaccharide-induced inflammatory response in human lens epithelial cells. *Invest Ophthalmol Vis Sci* 2006, 47:5395–5403
56. Brambilla R, Bracchi-Ricard V, Hu WH, Frydel B, Bramwell A, Karmally S, Green EJ, Bethea JR: Inhibition of astroglial nuclear factor kappaB reduces inflammation and improves functional recovery after spinal cord injury. *J Exp Med* 2005, 202:145–156
57. Messing A, Head MW, Galles K, Galbreath EJ, Goldman JE, Brenner M: Fatal encephalopathy with astrocyte inclusions in GFAP transgenic mice. *Am J Pathol* 1998, 152:391–398
58. Hagemann TL, Gaeta SA, Smith MA, Johnson DA, Johnson JA, Messing A: Gene expression analysis in mice with elevated glial fibrillary acidic protein and Rosenthal fibers reveals a stress response followed by glial activation and neuronal dysfunction. *Hum Mol Genet* 2005, 14:2443–2458
59. Foerch C, Curdt I, Yan B, Dvorak F, Hermans M, Berkefeld J, Raabe A, Neumann-Haefelin T, Steinmetz H, Sitzer M: Serum glial fibrillary acidic protein as a biomarker for intracerebral haemorrhage in patients with acute stroke. *J Neurol Neurosurg Psychiatry* 2006, 77:181–184
60. O'Callaghan JP, Sriram K: Glial fibrillary acidic protein and related glial proteins as biomarkers of neurotoxicity. *Expert Opin Drug Safety* 2005, 4:433–442
61. Fedoroff S, Vernadaskis A: *Astrocytes*. Orlando, Academic Press, 1986
62. Bush TG, Puvanachandra N, Horner CH, Polito A, Ostenfeld T, Svendsen CN, Mucke L, Johnson MH, Sofroniew MV: Leukocyte infiltration, neuronal degeneration, and neurite outgrowth after ablation of scar-forming, reactive astrocytes in adult transgenic mice. *Neuron* 1999, 23:297–308
63. Wyss-Coray T, Mucke L: Inflammation in neurodegenerative disease—a double-edged sword. *Neuron* 2002, 35:419–432
64. Tacconi MT: Neuronal death: is there a role for astrocytes? *Neurochem Res* 1998, 23:759–765
65. Mrak RE, Griffin WS: Interleukin-1, neuroinflammation, and Alzheimer's disease. *Neurobiol Aging* 2001, 22:903–908
66. Duncan AJ, Heales SJ: Nitric oxide and neurological disorders. *Mol Aspects Med* 2005, 26:67–96